AIAA ELECTRIC PROPULSION CONFERENCE
Broadmoor Hotel, Colorado Springs, Colo. March 11-13, 1963

17p.

ELECTRIC BREAKDOWN AND ARCING IN EXPERIMENTAL ION THRUSTOR SYSTEMS

by
John B. Stover
National Aeronautics and Space Administration
Cleveland, Ohio

63057-63

ELECTRIC BREAKDOWN AND ARCING IN EXPERIMENTAL ION THRUSTOR SYSTEMS

By John B. Stover
63057
Lewis Research Center
National Aeronautics and Space Administration
Cleveland, Ohio

20713

ABSTRACT

The importance of breakdown and arcing phenomena in ion thrustors arises both from the necessity to cluster modules to obtain useful thrust levels and from the probable advantages of the electrical paralleling of modules on a minimum number of power supplies.

An experimental program was undertaken to identify the breakdown and arcing phenomena in an electron-bombardment ion thrustor. Breakdown between the accelerating electrodes was observed below the levels determined by other investigators for either field emission from clean surfaces or sparking with surfaces contaminated by vacuum-pump oil, and well below the withstand voltage of the insulators. Following breakdown, self-extinction of low-current arcs frequently occurred, as expected from published reports on the instability of d-c vacuum arcs. A considerable percentage of the breakdowns, however, developed into sustained arcing. The low breakdown potential and the persistence of some low-current arcs both suggest the presence of contaminants on the electrodes. Luminous prebreakdown discharges observed at the electrodes tend to confirm the presence of contaminants.

AUTHOR

INTRODUCTION

Research on the electron-bombardment ion thrustor has progressed to the point where it is appropriate to consider system problems. For a given specific impulse there appears to be a limit to thrustor size, so that increases in thrust can be obtained only by a multiplicity of thrustor modules (ref. 1). Problems arising from the clustering of thrustor modules are under study, and an experimental investigation is presently being conducted at the Lewis Research Center. Figure 1 is a photograph of a three-module electron-bombardment ion thrustor array, which has been operated in a new 15-ft-diam., 60-ft-long vacuum tank at Lewis.

System problems arise because of the occurrence of electrical breakdown and consequent arcing between the high-voltage accelerating electrodes of the thrustor. Breakdown and arcing have been encountered frequently during basic thrustor research in the laboratory, where they have been no more than a nuisance. These arcing short circuits can be a major threat to the power system equipment for space missions, where power system equipment will necessarily have smaller weight and volume than the corresponding equipment in the laboratory and thus probably will be more vulnerable to the effects of arcing short circuits.

Arcing short-circuit problems will be intensified by clustering. It seems probable that minimum weight and complexity of power systems will be achieved by paralleling thrustor modules on a minimum number of power supplies. However, the rate of occurrence of arcing short circuits on a power supply should increase in proportion to the number of thrustors connected, so that a large number of thrustors in parallel on a single set

STOVER-1

of power supplies may be inoperative a large fraction of the time. Also, the maximum available short-circuit current will increase with the capacity of a power supply so that the destructiveness of arcing short circuits should increase with the number of thrustors in parallel on one set of supplies. Furthermore, repeated on-off cycling tends to reduce system lifetime and reliability. Thus, the proper method of handling electrical breakdowns and arcing short circuits, and the allowable number of parallel thrustors on one power supply, will be major considerations in the design of simple and reliable ion thrustor systems. Fundamental to these considerations is an understanding of the thrustor-initiated breakdown and arcing phenomena.

The investigation reported in this paper was concerned with the nature and general features of breakdown and arcing observed in single electron-bombardment ion thrustors and the associated power supplies. Probable causes of unusual features are discussed, and the implications for reliable operation of ion thrustor systems in space are pointed out.

BACKGROUND

Breakdown is defined herein as the onset of current between electrodes separated by a previously insulating medium and the accompanying rapid decrease in potential difference between the electrodes. Arcing is the subsequent conduction of current between electrodes at a small potential difference. Breakdown and arcing phenomena will be considered separately.

Breakdown in Vacuum

When the pressure of a gas between electrodes is reduced so far that the electron mean free path is of the order of the apparatus dimensions (about 10^{-3} mm Hg in the present case), the multiplication-by-collision process typical for low-pressure breakdown becomes very improbable. Experimental results show a leveling-off of breakdown voltage as pressure is reduced. At such pressures and below (a vacuum for the purposes of this discussion), other processes must be responsible for the observed breakdowns.

It has been established that, at sufficiently high field strengths near a cathode, electrons are accelerated through the potential barrier (work function) of the surface and travel to the anode. The electron emission resulting from the simple concept of high-field extraction through a work function barrier is presented in reference 2. This theoretical electron emission was found to be less than that observed experimentally, particularly for poorly outgassed surfaces. Thus, processes other than simple electron transmission across a work function barrier appear to be involved in vacuum breakdown.

Reference 3 reports breakdown at a potential difference of 100 kv between plane parallel electrodes, spaced 2 mm apart, in a continuously pumped vacuum system (with vacuum oil present, as it is in the vacuum facilities used for the present work). At 30 kv, prior to breakdown, 200-μa current transients of about 50-msec duration occurred across the 2-mm gap. The investigators felt that positive ions were formed in the gap and that the surfaces of the electrodes were covered by a contaminating layer of hydrocarbons, so that positive ions were more than replaced, upon their arrival at the cathode, by the production of negative ions. This process then increased into a current cascade that stopped

only when much of the contamination was removed from the electrode area involved in the discharge. The conditioning process was visualized by the investigators as the reduction of a grossly contaminated surface to one contaminated with a chemisorbed monolayer.

Reference 4 reports that breakdown of a vacuum gap at 5×10^{-3} mm Hg was initiated by the impingement of positive ions on a cathode, on which an insulating film of barium stearate (of the order of 10^{-5}-cm thickness) had been deposited. A positive ion current of the order of 10^{-8} amp was directed at the cathode. Breakdowns, followed by arcs, occurred at potentials from 34 to 2000 v for electrode spacings of 0.5 to 5.0 mm. Absence of either the film or the positive ion current eliminated breakdowns. One step of the mechanism postulated was that positive ions resting on the insulating film covering the cathode resulted in a high field at the cathode surface and that this high field caused field emission of electrons from the cathode. Consideration of the phases and duration of the observed arcs, as shown by oscillograms, suggested that neither the vapor of the electrode metal nor that of the film was involved in the initiation of the short-duration arcs that were observed. The same consideration suggested that the mechanism was completed by the arrival of positive ions obtained from adsorbed gas on the anode.

Arcing in Vacuum

Since the electron mean free path in vacuum is large compared with the dimensions of the apparatus, it follows that charge carriers required for arc current conduction cannot be generated in the residual gas. Current density at the cathode of the vacuum arc is exceedingly high (ref. 5), perhaps of the order of 10^5 or 10^6 amp/sq cm. This means that the vacuum arc is a "cold cathode" arc (i.e., the current density of the arc is too high to be attributed to thermionic emission from the cathode at its boiling temperature). The exact mechanism of current flow between the cathode, in which current flow is electronic, and the adjacent space between electrodes is not known. It is quite probable that the charge carriers required to conduct arc current are produced in the vapor of the electrodes, particularly in the vapor of the cathode, where the current density is very high. Diffusion of the vapor from the cathode spots into the adjacent lower pressure regions will result in a wide range of metallic vapor densities. It has been estimated (ref. 5) that an electron leaving the cathode would encounter densities corresponding to electron mean free paths between 10^{-5} cm at the cathode and several centimeters at the anode.

The results of a study of the stability of d-c vacuum arcs are contained in reference 6. The observed phenomenon of low-current arc chopping (abrupt cessation of current) was explained on the basis that a minimum density of metal vapor from the cathode must be required for a vacuum arc to exist. A value corresponding to about 10^{-3} mm Hg pressure was felt to be reasonable. The arc should chop if the cathode vapor diffused from the arc region and/or was produced in an insufficient quantity by a low-current arc.

In the experiments of reference 6 arc duration was measured by timing electrical noise of an arc drawn between clean, outgassed electrodes (3/4-in. diam. rods) of several materials in small-diameter (3-in.) tubes at various current levels. Results are illustrated in sketch (a), which

shows a very steep increase of average arc duration with current. Arc duration, at a given current, followed the survival law $N/N_o = e^{-t/\tau}$, where τ is the average arc duration and N/N_o is the fraction of arcs whose duration exceeded t. Arc stability was strongly affected by the vapor pressure of the electrode material. Refractory metals (tungsten and molybdenum), which require the highest temperatures to produce a given vapor pressure, had the most unstable arcs (the shortest average duration) at a given current level. (Symbols are defined in the appendix.) The data of sketch (a) were taken with minimal series inductance and shunt capacitance in the supply circuit. Thus, the data should reflect the stability of the arc itself and be relatively independent of complications because of circuit characteristics. The effect of inductance in the circuit is to increase average arc duration. For example, in an auxiliary test, reported in reference 6, an inductance of 3 mh in the circuit doubled average arc duration.

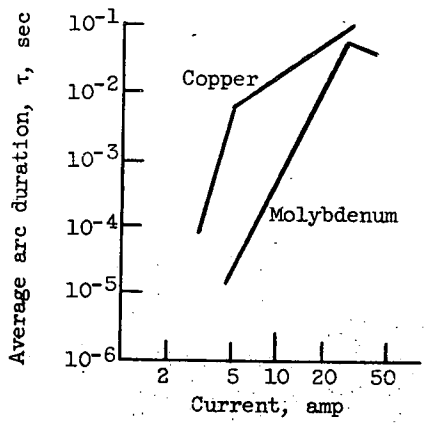

(a)

The voltage recovery characteristics of vacuum arcs are reported in reference 5. The investigation was a feasibility test of the use of a vacuum as a circuit-breaker dielectric. The recovery strength of the vacuum gap was tested by producing a half-cycle of 60-cycle arc current (at several hundred amperes, peak value) in an experimental vacuum circuit breaker. The external circuit was disconnected at the half-cycle current-zero time, and a high-voltage inverse pulse was applied after a time interval ranging from a few microseconds to several milliseconds after the current-zero time. A summary of the results of reference 5 is that most of the dielectric strength of the gap is recovered in less than 15 μsec. In many cases much shorter times were recorded, particularly for the lower peak values of the half-cycle arc current. It was reasoned that the rapid decrease in metallic vapor density in the interelectrode gap (by efflux of vapor to lower pressure regions) produced the rapid recovery of dielectric strength between the electrodes. These data on the rapid recovery of dielectric strength are useful in applying the average arc duration data of reference 6, which were obtained with currents that did not vary with time, to arc currents that do vary with time. Both arc duration and recovery of dielectric strength depend upon the density of metallic vapor in the interelectrode region. Thus, a rapidly decreasing arc current, such as one produced by a capacitor discharge, should have a predictable average duration at any given time, which should be no longer than that corresponding to the current magnitude that existed from 15 to 100 μsec earlier.

Stewart-4

APPARATUS AND PROCEDURE

Thrustor

Investigations of the electron-bombardment ion thrustor used in this investigation are reported in references 7 to 10. A cutaway sketch of the thrustor investigated is shown in figure 2. Mercury vapor is introduced into an ionization chamber, where it is bombarded by electrons emitted from a hot filament on the axis of the chamber. Rapid escape of electrons to the anode is prevented by an axial magnetic field. Escape of electrons to the ends of the chamber is prevented by operating these ends at the same potential as the filament. Positive ions and some neutral atoms diffuse from the plasma in the ionization chamber, and the ions are accelerated into the ion beam. The accelerating region is formed by two flat circular match-drilled molybdenum plates, which are separated by sapphire insulator balls seated in match-drilled holes at the periphery of the plates. These are called the screen and accelerator, or the accelerating electrodes. The thrustor body, of which the screen forms a part, is maintained at a high positive potential with respect to ground (typically 3500 v). The accelerator is held at a lesser negative potential with respect to ground (typically 1000 v).

The remainder of the thrustor with the exception of the magnetic field coil and filament is fabricated of nonmagnetic stainless steel. A schematic diagram of the thrustor and its power supplies is shown in figure 3.

Vacuum Tank Facility

Figure 4 shows a sketch of the vacuum facility. The 5-ft-diam., 16-ft-long tank has three 32-in. oil diffusion pumps feeding into a common ejector pump, followed by a mechanical pump. With cryogenic pumping used in conjunction with the previously mentioned pumps, tank pressures in the 10^{-6} mm Hg pressure range were obtained during thrustor operation. The facility is described in greater detail in reference 11. The thrustor was mounted either inside the tank or in a 20-in.-diam. bell jar that opened to the tank through a 12-in. valve.

Power Supply Circuits

Information on the response of the power supplies to short circuits between the screen and accelerator plates of the thrustor is necessary in order to understand the oscillograms that will be presented. In figure 3, the power supplies of interest are those marked V_I and V_A. Initially the short-circuit response is governed by the filter capacitors of both power supplies and the resistance between them. The partial circuit that controls the initial response is shown in sketch (b).

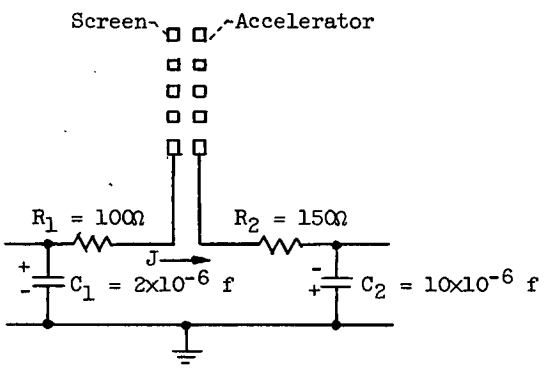

(b)

The initial current response is as shown in sketch (c). The current is

initially near zero. Following the breakdown, the current rises rapidly to a peak value and then decays. The time constant of the current decay is about 0.4 msec. Current rise time is about 10 μsec, which is too

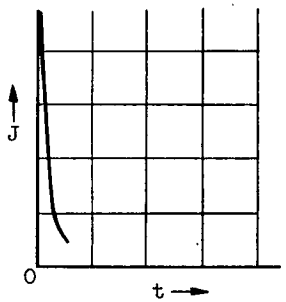

(c)

short to be shown in sketch (c). The initial voltage transient from the shorted electrodes to ground is of roughly the same shape as the current decay.

The behavior becomes more complicated after the initial response as the inductance and resistance of the power supplies shown in sketch (d), the completed equivalent circuit diagram, also affect the response. The

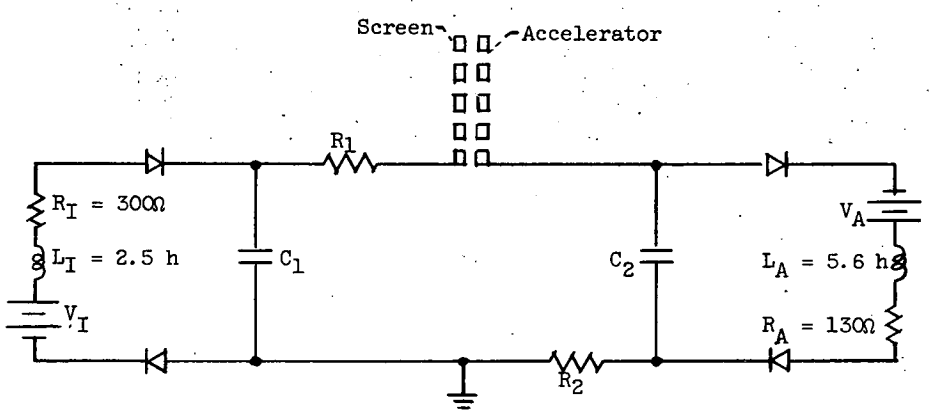

(d)

sustained short-circuit current, however, does follow the general form of current buildup in a series resistance and inductance. The values of the inductance and resistance are such that the time constant of the current buildup is about 10 msec. Sketch (e) shows the general trend of the completed short-circuit current response. The ultimate value of the cur-

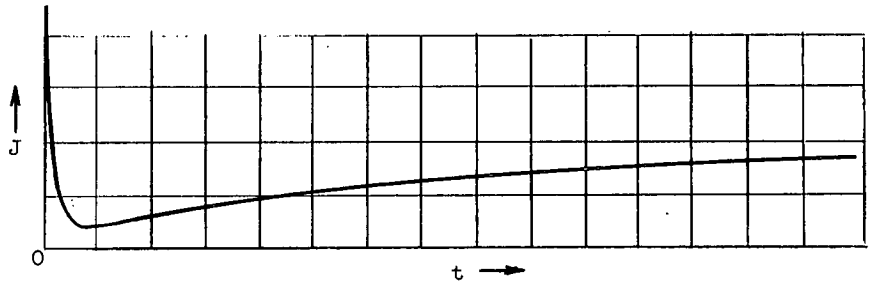

(e)

rent is controlled by the total circuit resistance and the sum of the voltages applied to the electrodes. The ultimate voltage level of the electrodes with respect to ground depends upon the relative values of the two voltages initially applied and the relative values of resistance between each electrode and ground. In the circuit used during this work, the ultimate voltage to ground was about 850 v (for initial values of V_I = 3500 and V_A = 1000). A reapportionment of resistance between the two power supplies could have resulted in a different value - even in a negative ultimate voltage to ground. The initial and ultimate voltage response is roughly similar to the current response.

Initial capacitor discharge arc currents have been observed to chop to zero current on the tail of the wave. When this occurs, the respective capacitors of each power supply recharge through series inductance and

resistance. The resulting voltage waveform following a chopped current is approximately as shown in sketch (f). The circuit parameters are of such values that the screen voltage recovery is faster than the accelerator voltage recovery. Only the screen voltage recovery wave is shown. The dotted part of the wave beyond the first maximum does not actually

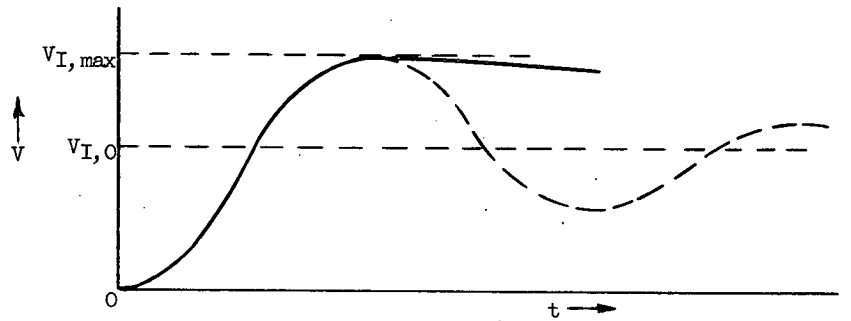

(f)

occur because of the presence of rectifier elements. The maximum voltage persists because the maximum charge delivered to the capacitor is trapped there by these rectifier elements. Electrode voltage can only return to its original level by partial discharge of the capacitor (by way of beam current, e.g.).

Procedure

Breakdown potential at various pressures with the thrustor not operating was measured in the bell jar of the 5-ft-diam. tank, with the bell jar open to the tank. With the accelerator electrode grounded, the screen potential was increased until sustained arcing occurred, and the power supply was shut off by operation of a relay and a circuit breaker. Several breakdowns were initiated in this way at each pressure level. Spacing between the molybdenum screen and accelerator electrodes was 2 mm. The background gas was air. There was no mercury in the thrustor boiler. The pressure in the bell jar was reduced in steps from atmospheric pressure to about 10^{-6} mm Hg. First the throttled mechanical pump was operated alone, and then the ejector pump was added. Finally the diffusion pumps were operated with a controlled leak from atmosphere to the tank. A pressure range of nearly nine decades was spanned in this way. Pressure in the bell jar was measured successively on a Bourdon gage, thermocouple gage, and an ionization gage. Breakdown potential was measured with the power supply voltmeter (2-percent accuracy) and with a portable voltmeter at the lower voltage levels.

Oscillograms were also made of arc current and electrode voltage excursions following breakdowns that occurred spontaneously during normal thrustor operation. The thrustor was started by setting inlet steam pressure at about 2 in. water gage to obtain a known flow of mercury vapor through a previously calibrated boiler orifice. The magnetic field current was set, and a discharge was started in the ionization chamber by supplying filament heater current and anode potential. Accelerating voltages were applied to the screen and accelerator plates. Ion beam current, as indicated by the ground return meter labeled J_B in figure 3, was set to the desired level by controlling the filament emission current. Neutralization was not controlled but depended on the natural processes of ionizing neutrals in the tank and the secondary emission of electrons from the target to supply electrons.

Half-ohm resistors were installed as current shunts in the ground side of each high-voltage accelerating electrode power supply and were

connected to an oscilloscope to signal arc current excursions. Ten-megohm potential dividers were connected directly between accelerating electrodes and ground. The dividers were connected to an oscilloscope to signal potential excursions. Most of the oscillograms were made on dual-beam oscilloscopes equipped with differential amplifiers. Spontaneous breakdowns were recorded by setting the scope for automatic single-sweep operation, internally triggered, usually by the rise of arc current rather than by the collapse of electrode voltages.

RESULTS AND DISCUSSION

Breakdown with Nonoperating Thrustor

It has been reported in reference 12 that breakdown with ion and propellant flow occurs at potentials somewhat below those at which breakdown without ion or propellant flow occurs and that these potentials appear to be related. Nonoperating breakdown measurements can be made over a much wider range of pressures than those at which thrustors can be operated. They therefore can reveal trends and features that cannot be observed during thrustor operation.

Figure 5 shows the breakdown voltage of the nonoperating electron-bombardment ion thrustor as a function of pressure. To the right of the minimum the thrustor curve follows the familiar Paschen curve for air for the same spacing as that between the accelerating electrodes of the thrustor. It is reasonable that the minimum should be extended to lower pressures because the field of the high-voltage thrustor body extends to the grounded tank and accelerator electrode, as well as between the screen and accelerator electrodes. This permits long-path discharges to occur at the minimum breakdown potential, or somewhat above, at pressures well below those corresponding to the minimum for direct paths between the parallel electrodes. As the range of long paths becomes exhausted, the curve turns upward, as does the simple-path Paschen curve for air. In the lower pressure regions, surface effects dominate the breakdown phenomena, and the breakdown voltage becomes independent of pressure. The plateau of figure 5, on the left, shows this independence of pressure.

At voltages somewhat below the breakdown voltage in the 10^{-5} mm Hg pressure range, a steady luminous discharge was observed at the surface of the accelerator electrode. This discharge occurred both with and without the engine body mounted on the electrode assembly. It appeared as a dull blue glow, nonuniformly, over the visible portion of the accelerator electrode. It was further evidenced by a small current ($\approx$1 ma) between plates and to ground. There was no mercury in the thrustor boiler at the time these observations were made; however, the vacuum tank had a history of heavy mercury loading from the ion thrustor experimental program. Similar observations of prebreakdown discharge were made on a new thrustor mounted in a new 15-ft-diam., 60-ft-long vacuum tank, which had no history of mercury loading. Again a dull blue glow was observed. It was difficult to assign any specific location to it because it was less intense than the previously observed glow. Time-exposure color photographs showed that the blue glow was in fact present and that the discharge was either between the accelerator plates or behind them (possibly inside the ionization chamber of the thrustor, although it was not

operating during these tests). Breakdown voltage in this case was 4.4 kv with an electrode spacing of 1.4 mm. The similar results for a new thrustor and tank indicated that accumulated mercury deposits were not involved, although other electrode contaminants could still be responsible.

In the electron-bombardment ion thrustor the accelerating electrodes are spaced and positioned by means of several sapphire balls, about 3/16-in. in diameter in the static breakdown tests, seated in matching holes at the periphery of the flat circular accelerator plates. Separate tests of 3/16-in.-diam. sapphire balls positioned in matching holes between flat plates (about 3.3 mm apart) in vacuum of 10^{-5} mm Hg showed that they are capable of withstanding 24 kv at room temperature. At 330° F the withstand potential is still 16 kv (unpublished NASA data). Hence, it appears that the insulator balls do not play a primary role in determining the nonoperating breakdown potential.

The flat-plate accelerator electrodes are match-drilled in order that propellant ions may be focused through the holes by the electric field and exhausted from the thrustor. To test the effect of electric field nonuniformity introduced by these holes upon the breakdown level, a set of undrilled plates was mounted on the thrustor used to determine the breakdown voltage curve of figure 5. Average breakdown voltage comparison at 10^{-6} mm Hg pressure in the bell jar of the 5-ft-diam. vacuum tank was about 30 percent higher with a spacing between electrodes 20 percent greater than with the perforated plates. Thus, the breakdown electric field was nearly the same for the two tests, and the holes apparently had little effect on breakdown. After the tests, the accelerator electrodes had bright, clean spots on the surfaces that faced each other across the vacuum gap. These spots were about 1 in. in diameter, generally round, and were located at about a half radius from the centers of the plates.

Comparing these results with previous work from references 3 and 13 shows some disagreement. Reference 13 predicts a minimum breakdown voltage of 30 kv for a 2-mm gap in vacuum with nonoutgassed electrodes. Reference 3 reports frequent current transients at 30 kv across a 2-mm gap in a continuously pumped vacuum system, with breakdown at 100 kv. A possible explanation of the differences in breakdown and prebreakdown voltages is contained in reference 4. As described previously, reference 4 reports that breakdowns, followed by arcs, occurred at potential differences below 2000 v for electrode spacings up to 5 mm if a small positive ion current impinged on a thin insulating film present on the surface of the cathode. However, it is not known if enough positive ions were available to the thrustor accelerator plate of these nonoperating tests to lead to the type of breakdown described in reference 4.

In summary, the maximum breakdown voltage of the nonoperating ion thrustor was considerably below the level that should be expected in continuously pumped vacuum systems. Neither the sapphire insulating balls nor the field nonuniformities introduced by the drilled holes in the accelerating electrodes can be held responsible for limiting the breakdown voltage. The luminous prebreakdown discharges observed suggest the presence of outgassing contaminants on the accelerating electrodes. These contaminants, which appear to be more severe in the pres-

ent system than in those of references 3 and 13, are probably responsible for the reduction of thrustor breakdown voltage below the level obtained by other investigators.

Breakdown During Operation

Operational experience with ion thrustors has shown that new accelerator electrodes break down and arc at voltages considerably below the design voltage. It is only after a period of arc-conditioning that they can be operated with any degree of stability at the design potentials. Arcing short circuits every minute for the first hour of operation are typical with new accelerator plates. After this initial conditioning period there is a shorter period of unstable operation, say 10 min, each time a thrustor is started after being exposed to atmospheric pressure. The longest period free of sustained arcing attained to date at Lewis has been 25 hr during a 150-hr endurance run.

Visual observations of the screen and accelerator plate region during thrustor operation indicate that there are at least two types of breakdown that lead to sustained arcing on the power supply. These are distinguished by the type of the arc that follows breakdown. One is indicated by a streamer about 1 in. long, which appears to bridge the gap at the periphery of the accelerator plates curving somewhat outward from the periphery of the plates. This streamer circles the thrustor in the field of the magnet coil. The direction of rotation reverses when the direction of the magnetic field is reversed. The streamer usually travels about a third of the circumference, about 10 cm. The arc lasts about 1/5 sec, which indicates an arc speed of about 50 cm/sec. Arcs of this type were always followed by operation of the power supply circuit breaker. The second type of arc, following breakdown, occurs near the center of the accelerator plates and apparently between the screen and accelerator electrodes. This is a short brilliant arc rather than a thin streamer. Arcing that was not sustained, and therefore did not result in the operation of a circuit breaker to shut off the power supply, was apparently always of the second type although usually less brilliant than those arcs that operated the circuit breaker.

Data have been reported which show a general increase in breakdown voltage with the length of gap between the screen and accelerator plates (ref. 12). Breakdown was more dependent upon the total voltage between electrodes than upon the individual voltage of either electrode. No general dependence of breakdown voltage upon beam current level or upon rate of neutral propellant flow was found.

Calculation of the maximum possible neutral (Hg) flow with a beam current of 0.5 amp from a 10-cm-diam. thrustor yields a number density in the interelectrode gap corresponding to a pressure of 5×10^{-4} mm Hg. Figure 5 shows that this overall pressure of air would not result in breakdown below 10 kv. Also shown on figure 5 are the data of reference 14, which give the lower leg of the Paschen curve for both air and mercury. Although data for air do not agree with other data, also shown, the direct comparison between air and mercury by the same investigator is of interest. The point to note is that to the left of the Paschen minimum point mercury is comparable with air, if not superior, in breakdown voltage. Therefore, it seems improbable that the maximum density of

neutrals (Hg) that can be in the interelectrode gap will lead to breakdown.

There is a strong possibility that the insulating film mechanism suggested in reference 4 is operative in breakdown during thrustor operation when both charge-exchange and poorly focused beam ions can impinge on the electrodes. The most likely insulating film is molybdenum trioxide, MoO_3. Oxide films form readily on molybdenum in air or oxygen at temperatures of the order of 200° C. A previously formed film begins to evaporate in a vacuum of 10^{-6} mm Hg when heated to 415° C, but the rate of vacuum oxidation still exceeds the evaporation rate (ref. 15). The temperature of accelerator electrodes during thrustor operation is about 250° C. It seems reasonable to expect that molybdenum trioxide was present as insulating film on the electrodes. There can also be films of adsorbed gas, and initially at least, films of grease and dirt. The breakdown mechanism suggested in reference 4 seems consistent with the conditions under which the thrustor breaks down during operation and is proposed as a working hypothesis for further investigation.

Arcing

Figure 6 is a tracing of an oscillogram of electrode current and simultaneous voltage-to-ground excursions of the screen electrode for a breakdown that developed into sustained arcing. In this instance the thrustor was operating at a beam current of 0.13 amp with the screen (V_I) at +3500 v and the accelerator (V_A) at -1000 v with respect to ground. The gap between electrodes broke down at 4500-v potential difference. The accelerator voltage source recharged its capacitor through a larger inductance than did the screen voltage source, whose variation is shown in figure 6, so that the variation of V_A was slower and did not exceed 500 v during the excursions of V_I.

The initial breakdown was followed by a capacitor discharge arc, which appears on the upper trace of figure 6. The rise time of the capacitor discharge arcs was about 10 μsec, so the rate of current rise was of the order of 10^6 amp/sec. This arc current chopped and was extinguished at a current level somewhat under 2 amp. This chopping occurred, as described previously, because the metal vapor required for the existence of the arc diffused into lower pressure regions too rapidly for the arc to be sustained. The second breakdown occurred at about 4500 v on the overswing of V_I as the discharged capacitor was recharged through the power supply inductance. This was followed by a second capacitor discharge arc, which again chopped. A third breakdown then occurred at about 5300 v. The capacitor discharge arc that followed did not chop but underwent a transition to a sustained arc. The sustained arcing was terminated by operation of a relay and circuit breaker that shut off the power supply. The breakdown and arcing illustrated by the oscillograms in figure 6 are typical of the class of capacitor discharge arcs that result in sustained arcing. The number of capacitor discharge arcs preceding the transition varies from one, in which case no chopping or overvoltage swings occur at all, to a dozen or more.

The second class of arcs is that in which occurred one or several combinations of breakdown followed by a final capacitor-discharge arc that chopped at low current and did not result in a transition to a

STOVER-11

sustained short circuit on the power supply. Figure 7 shows oscillogram traces of the initial arc current excursions of both classes. These four oscillograms were taken during the operation of one thrustor within a period of about 1 hr. Those on the left developed into sustained arcing and were terminated by operation of a relay and circuit breaker that shut off the power supply; those on the right occurred without resulting in sustained arcing. An interesting point to note is the gradual nature of the "chop" on the oscillogram on the upper right. It is possible that such a gradual chop terminated the last arc of each series that did not develop into sustained arcing, thereby damping the overswing of voltage on the condenser. An oscillogram trace of the voltage ($V_I + |V_A|$) excursion during such a nonsustained arc is shown in sketch (g). It indicates that the vacuum gap may sometimes be strong enough to withstand the overvoltage following capacitor discharge arcs. The initial value of ($V_I + |V_A|$) was 5 kv, as indicated by the dotted line in sketch (g).

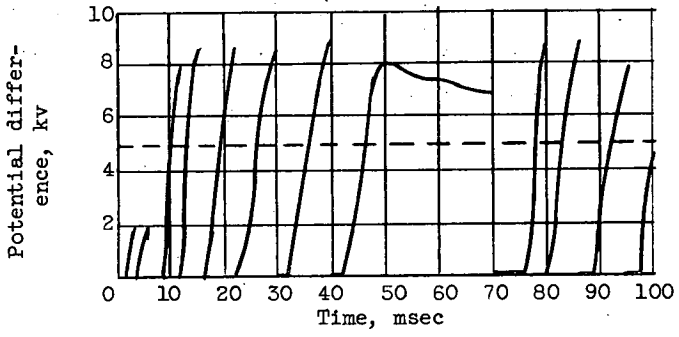

(g)

Many of the arcs observed during this investigation were of this second type (self-clearing without subsequent sustained arcing). Some work was done to determine the relative number of each class of arc by using electronic counters, but the techniques used were not sufficiently well developed to yield satisfactory data. It is believed, however, that the proportion of nonsustained arcs was high (well above 50 percent).

It seems clear from the data of references 5 and 6 that the basic phenomenon to be expected after breakdown and subsequent capacitor discharge arcing is the chopping of arc current at a low current level and the rapid recovery of strength by the vacuum gap (in some tens of microseconds).

The question therefore arises: What factor is responsible for the persistence of low-current arcs that lead to sustained arcing? This persistence is illustrated in figure 6, where the third capacitor discharge arc current turns up and becomes a sustained arc. The two pairs of oscillogram tracings in figure 7 show that the turnup of the capacitor-discharge arc current is observed both in the case where a sustained arc ultimately develops, on the lower left trace, and where a sustained arc does not develop, on the lower right. However, when a sustained arc does occur, the turnup persists. There seem to be two possibilities to explain the persistence of low currents on the refractory (molybdenum) electrodes in vacuum. First, the voltage recovery characteristics of the two power supplies are such that electron back streaming from the ion-beam target can occur during recovery from an arc. However, the magnitude of the possible back-streaming current is far too low to maintain a vacuum arc.

The second possible explanation of low-current persistence is that adsorbed gas or other contaminants may provide additional charge carriers under the scouring and local heating action of the capacitor discharge arc. A monolayer of adsorbed gas atoms or molecules has a surface number density of 10^{14} to 10^{15} per square centimeter. Under the heating and impingement of an arc, a volume number density of at least 5×10^{14} per cubic centimeter could be produced (equivalent to about 10^{-2} mm Hg pressure). It is quite likely that more than a single molecular layer of gas, or other contaminants, is present on the electrode surfaces. The luminous discharges observed during the work on static breakdown suggest the presence of considerable contamination. It seems likely that such contamination provides the additional charge carriers necessary to cause persistence of low-current arcs that result in sustained arcing on the power supplies.

CONCLUDING REMARKS

Design of simple and reliable power systems with many thrustor modules connected in parallel on a single power supply depends on an understanding of breakdown and arcing phenomena that occur in individual thrustors. The nature and general features of breakdown and arcing in experimental electron-bombardment ion thrustor systems have been presented in this paper.

For the nonoperating thrustor, breakdown between accelerating electrodes occurred at potentials too low to be attributed to field emission or to the presence of hydrocarbons in the continuously pumped vacuum system. Luminous prebreakdown discharges were observed which suggest that contaminants on the electrodes may be responsible for the low breakdown potential.

For the operating thrustor, breakdown potential is further reduced. Calculations indicate that propellant densities existing in the interelectrode region are too low to account for this breakdown. The possibility that breakdown is caused by a high field at the cathode resulting from the collection of positive ions on a thin nonconducting contaminant film on that electrode seems worthy of further investigation.

It seems clear that instability and self-extinction of low-current arcs should occur following breakdown, with low-inductance circuits. Self-extinguishing arcs have been observed, but there is also a large number of arcs that persist and result in sustained arcing. It is suggested that persistence of low-current arcs can be attributed to the generation of additional charge carriers from films of contaminants on the accelerating electrodes.

Substantial reduction of the rate of occurrence of breakdown, and the promotion of the self-extinguishing characteristics of arcs that do occur, can contribute to the simplicity and reliability of ion thrustor power systems. It is possible that more ideal breakdown and arcing characteristics will be realized in the space environment after relatively simple prelaunch and postlaunch thrustor-conditioning techniques have been developed. Further investigation should be undertaken to attain these more ideal characteristics in ground facilities.

APPENDIX - SYMBOLS

C_1, C_2	capacitances, farads
J	current, amp
J_A	accelerator impingement current, amp
J_B	ion beam current, amp
L_A	inductance of accelerator high-voltage power supply, h
L_I	inductance of screen high-voltage power supply, h
N	number of arcs with duration less than a given period, dimensionless
N_o	total number of arcs, dimensionless
R_A	equivalent resistance of accelerator high-voltage power supply, ohms
R_I	equivalent resistance of screen high-voltage power supply, ohms
R_1, R_2	resistances, ohms
t	time, sec
V	potential, v
V_A	potential of accelerator electrode, v
ΔV_F	potential difference across filament heater, v
V_I	potential of screen electrode, v
ΔV_I	potential difference between anode and filament in ionization chamber, v
$V_{I,max}$	maximum potential of screen electrode, v
$V_{I,o}$	operating potential of screen electrode, v
ΔV_M	potential difference across magnetic-field coil, v
	average duration of d-c vacuum arc at a given current, sec

REFERENCES

1. Kaufman, Harold R.: The Electron-Bombardment Ion Rocket. Paper Presented at Third Symposium on Advanced Prop. Concepts, AFOSR and General Electric Co., Cincinnati (Ohio), Oct. 1962.
2. Loeb, Leonard B.: Basic Processes of Gaseous Electronics. Univ. Calif. Press, 1960.
3. Mansfield, W. K., and Fortescue, R. L.: Pre-Breakdown Conduction Between Electrodes in Continuously-Pumped Vacuum Systems. British Jour. Appl. Phys., vol. 8, 1957, pp. 73-78.
4. Haworth, F. E.: Experiments on the Initiation of Vacuum Arcs. Phys. Rev., vol. 80, no. 2, 1950, pp. 223-226.
5. Cobine, J. D., and Farrall, G. A.: Recovery Characteristics of Vacuum Arcs. Paper CP 62-139, Am. Inst. Elec. Eng., 1962.
6. Cobine, J. D., and Farrall, G. A.: Experimental Study of Arc Stability, I. Jour. Appl. Phys., vol. 31, no. 12, Dec. 1960, pp. 2296-2304.
7. Kaufman, Harold R.: An Ion Rocket with an Electron-Bombardment Ion Source. NASA TN D-585, 1961.
8. Kaufman, H. R., and Reader, P. D.: Experimental Performance of an Ion Rocket Employing Electron-Bombardment Ion Sources. Paper Presented at Nat. IAS-ARS Joint Meeting, Los Angeles (Calif.), June 1961.
9. Reader, Paul D.: Investigation of a 10-Centimeter-Diameter Electron-Bombardment Ion Rocket. NASA TN D-1163, 1962.
10. Kerslake, William R.: Accelerator Grid Tests on an Electron-Bombardment Ion Rocket. NASA TN D-1168, 1962.

Stowe 14

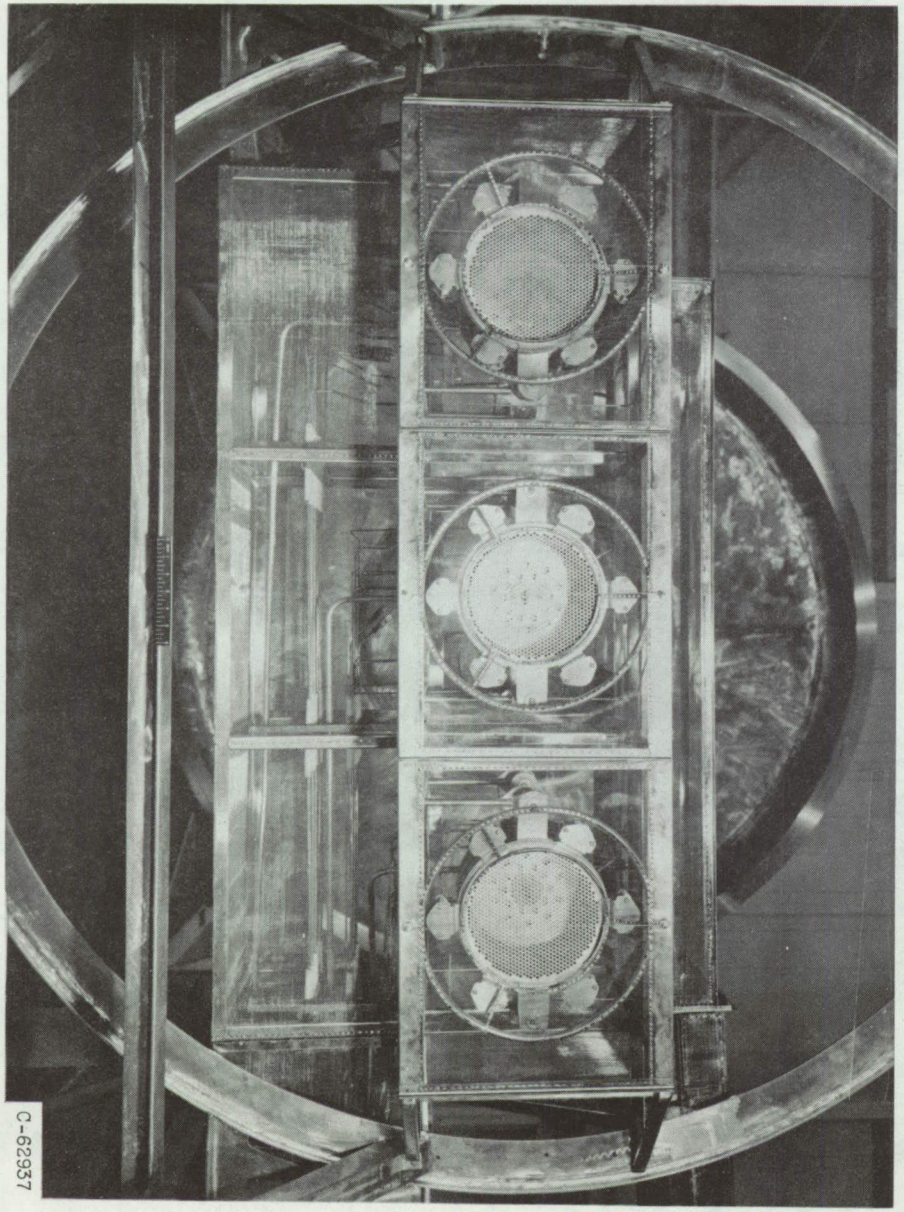

C-62937

Figure 1. - Three-module array of 20-centimeter-diameter electron-bombardment ion thrustors mounted in 15-foot-diameter vacuum tank at Lewis Research Center.

11. Keller, Thomas A.: NASA Electric Rocket Test Facilities. Seventh Nat. Symposium on Vacuum Tech. Trans., Pergamon Press, 1960, pp. 161-167.

12. Kerslake, William R.: Charge-Exchange Effects on the Accelerator Impingement of an Electron-Bombardment Ion Rocket. NASA TN D-1657, 1963.

13. Hawley, R.: Vacuum as an Insulator. Vacuum, vol. 10, 1960, pp. 310-318.

14. Guseva, L. G.: Initiation of a Discharge in Molecular Gases at $(pd) < (pd)_{min}$. Trans. All-Union Inst. Elec. Eng. No. 63, State Pub. House for Energetics, B. N. Klyarfel'd, ed., Moscow & Leningrad, 1958. (Trans. available from Liason Office, Tech. Info. Center, MCLTD, Wright-Patterson Air Force Base, Ohio.)

15. Kohl, Walter H.: Materials and Techniques for Electron Tubes. Reinhold Pub. Co., 1960.

16. Cobine, James Dillon: Gaseous Conductors. Dover Pub., Inc., 1958.

STOVER-15

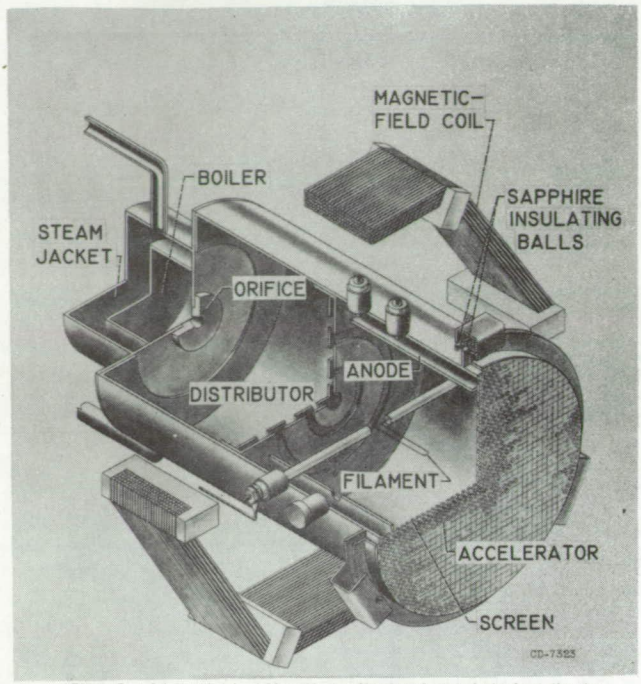

Figure 2. - Cutaway sketch of 10-centimeter-diameter electron-bombardment thrustor.

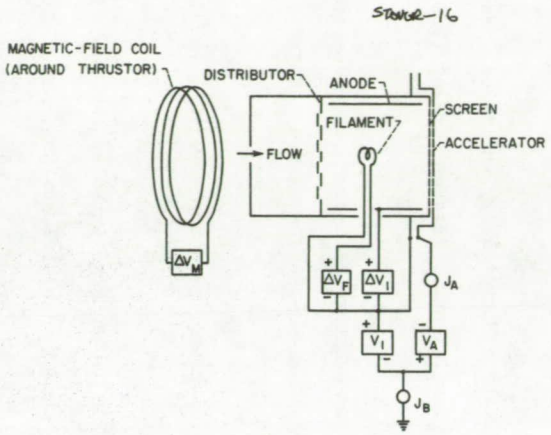

Figure 3. - Schematic diagram of electron-bombardment thrustor and electric power supplies.

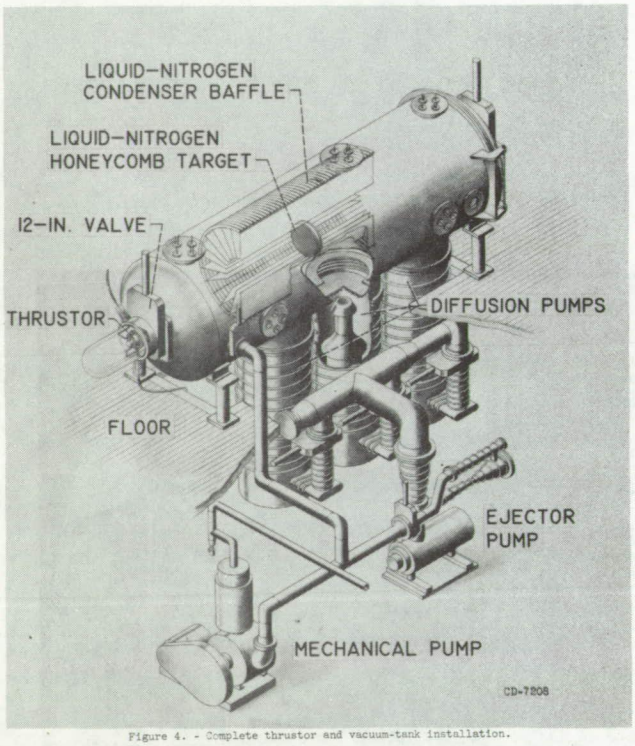

Figure 4. - Complete thrustor and vacuum-tank installation.

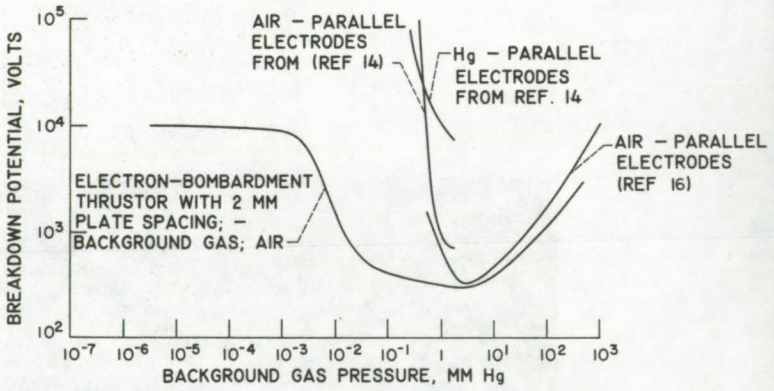

Figure 5. - Non-operating electron-bombardment ion thrustor breakdown potential variation with background air pressure.

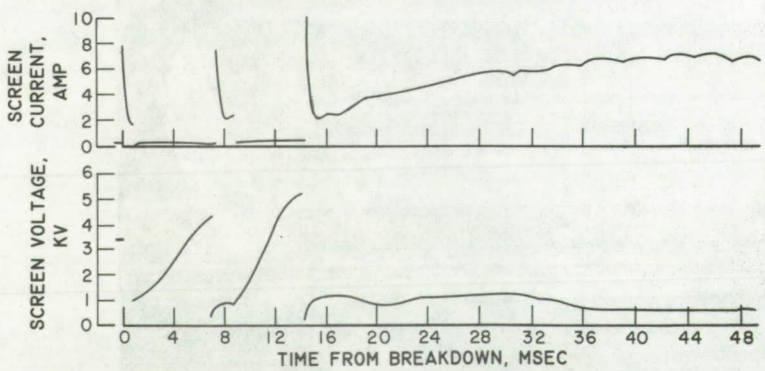

Figure 6. - Screen electrode current and potential excursions following breakdown between screen and accelerator electrodes during operation of electron-bombardment ion thrustor.

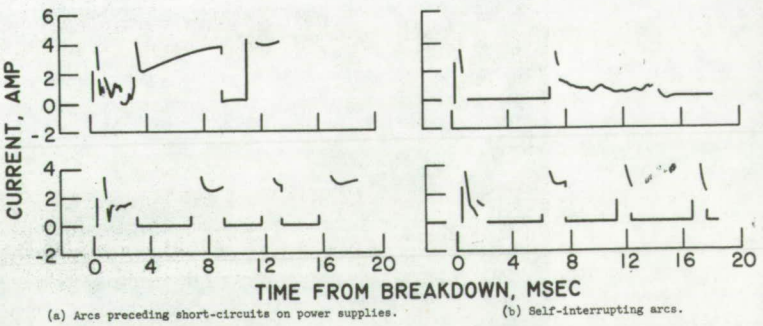

(a) Arcs preceding short-circuits on power supplies. (b) Self-interrupting arcs.

Figure 7. - Oscillograms of capacitor-discharge-controlled arc currents from screen electrode of operating electron-bombardment ion thrustor.

12. Head, R. M.: Investigations of Spontaneous Condensation Phenomena. Ph.D. Thesis, C.I.T., 1949.

13. Tolman, Richard C.: The Effect of Droplet Size on Surface Tension. Jour. Chem. Phys., vol. 17, 1949, pp. 333-337.

14. Loeb, Leonard B.: Fundamental Processes of Electrical Discharge in Gases. John Wiley & Sons, Inc., 1939, p. 149.

15. Cahn, Lee, and Schultz, Harold K.: Vacuum Microbalance Techniques. Vol. 2. Plenum Press, 1962, p. 7.

16. Glasstone, S : Textbook of Physical Chemistry. D. Van Nostrand Co., Inc., 1946, p. 492.

17. Reid, Robert C., and Sherwood, Thomas K.: The Properties of Gases and Liquids. McGraw-Hill Book Co., Inc., 1958, p. 7.

18. Lange, Norbert A.: Handbook of Chemistry. Fifth ed., Handbook Publ., Inc., 1944, p. 210.

19. Hodgman, Charles D., ed.: Handbook of Chemistry and Physics. Thirty-eighth ed., Chem. Rubber Pub. Co., 1956-1957, p. 550.

20. Anon.: A comprehensive treatise on inorganic and theoretical chemistry. Longmans Green and Co., London, England, 1946, p. 802.

21. Perry, John H.: Chemical Engineers Handbook. Second ed., McGraw-Hill Book Co., Inc., 1941, p. 633.

TABLE I. - PHYSICAL PROPERTIES OF MERCUROUS CHLORIDE

Property	Units	Value	Reference
Molecular weight	amu	236.07	18
Density	$grams/cm^3$	7.15	18
Melting point	^oC	302	18
Sublimation point	^oC	373	19
Boiling point	^oC	382.5	18
Latent heat of vaporization at-	$\frac{gram\text{-}cal}{gram}$		20
16^o C		131	
18^o C		127	
Specific heat ratio	$\gamma = c_p/c_v$	1.33	21

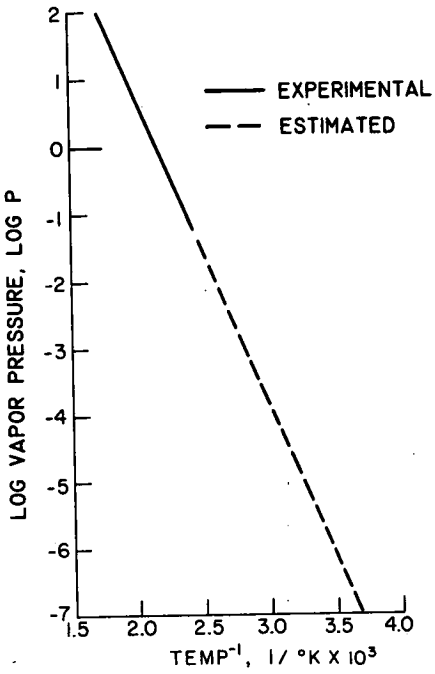

Figure 1. - Variation of mercurous chloride vapor pressure with temperature. Experimental data from Lange, N.A., "Handbook of Chemistry." Handbook Pub., Inc., 1944 p. 1429.

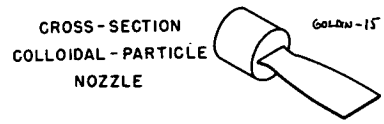

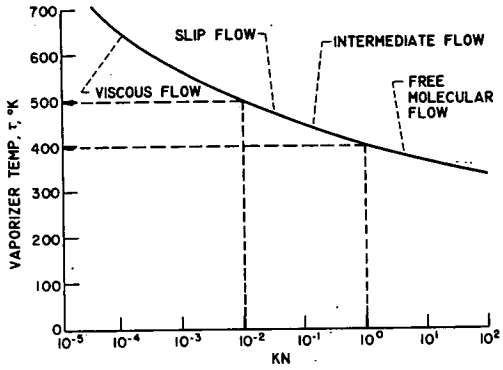

(a) Knudsen number.

Figure 2. - Flow regimes in colloidal particle generator. Propellant, mercurous chloride.

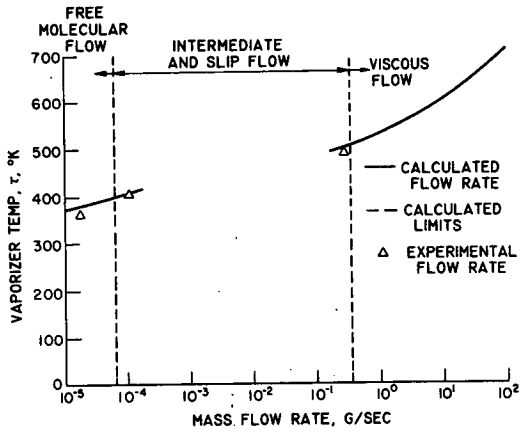

(b) Mass flow rate.

Figure 2. - Concluded. Flow regimes in colloidal particle generator. Propellant, mercurous chloride.

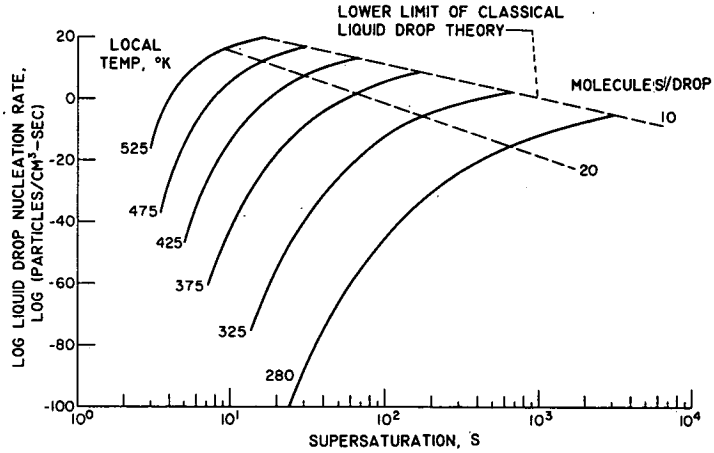

Figure 3. - Classical liquid drop nucleation rate for mercurous chloride.

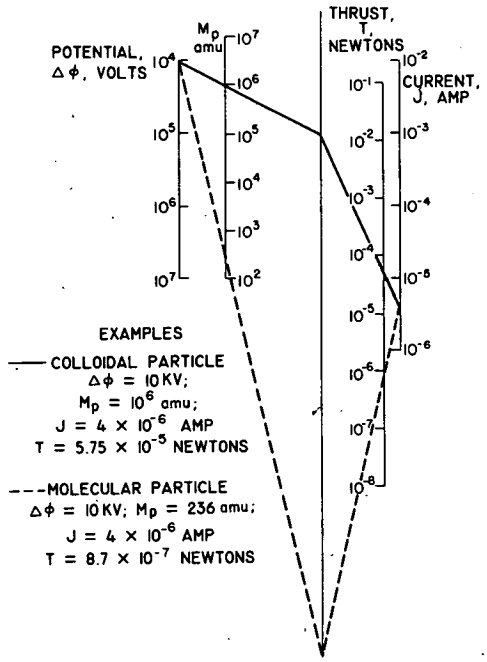

Figure 4. - Thrust of colloidal particle thrustor with singly charged particles.
$T = 1.44 \times 10^{-4}\ J K_p^{1/2} \Delta\phi^{1/2}$

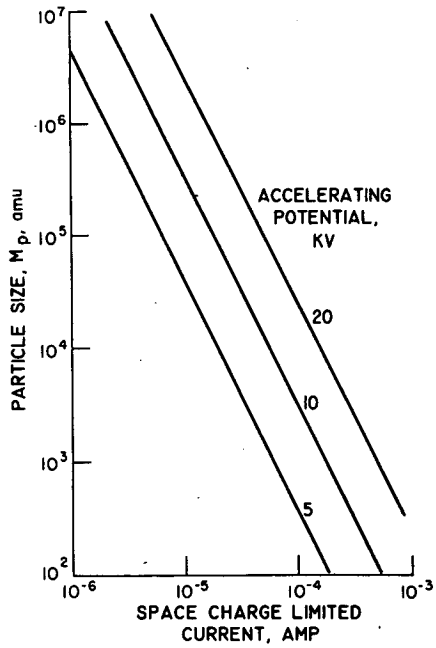

Figure 5. - Child's law current for the experimental colloidal thrustor with singly charged particles. Accelerator length, 4.2 cm; beam area, 2 cm^2.

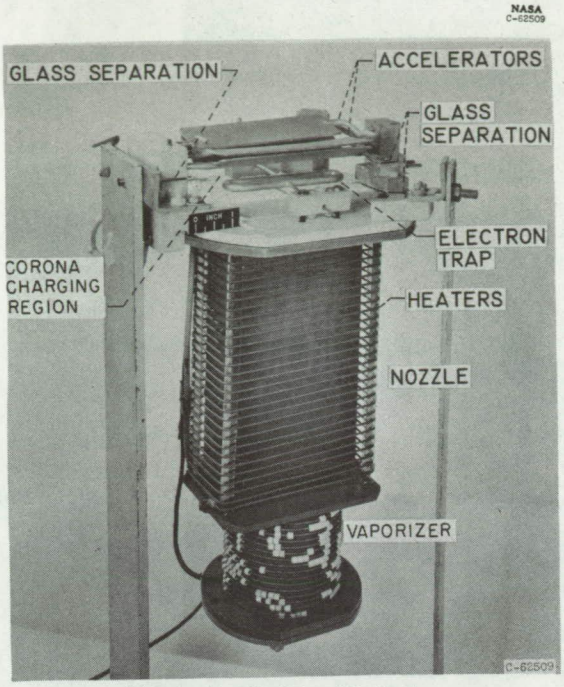

(a) Condensation colloidal particle thrustor.

Figure 6. - Experimental Colloidal Test set-up.

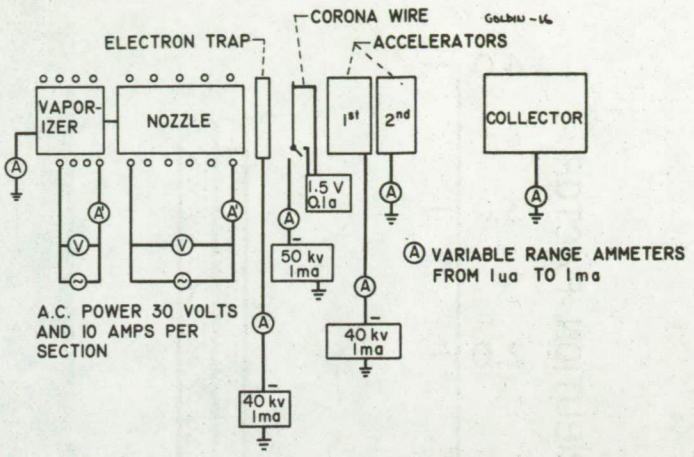

(b) Power supply and metering system.

Figure 6. - Concluded. Experimental Colloidal Test setup.

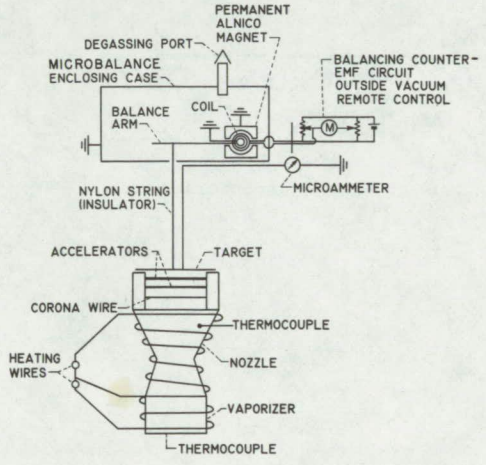

Figure 7. - Experimental thrust monitoring set-up for colloidal particle thrustor.

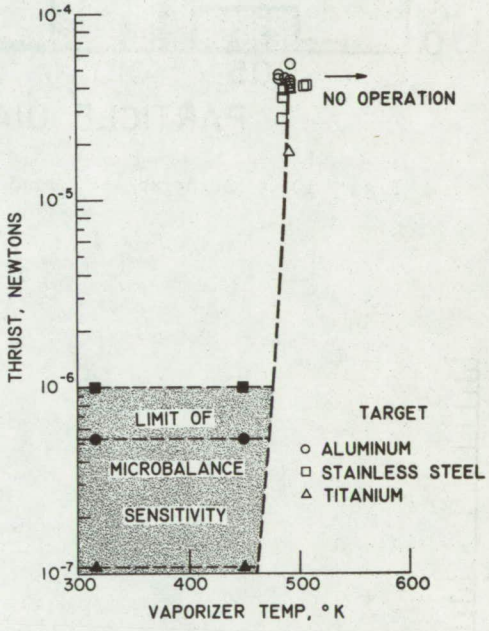

Figure 8. - Experimental thrust measurements of the colloidal thrustor. Accelerating potential 10-12 kv; collector current 0-6μa. Propellant, mercurous chloride.

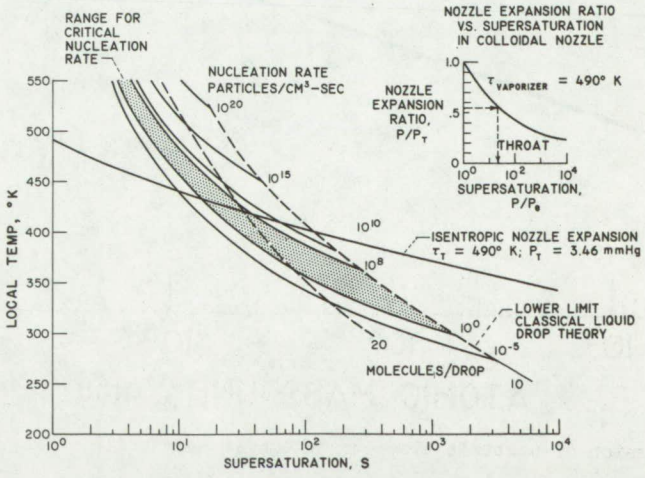

Figure 9. - Critical supersaturation for colloidal nozzle. Propellant, mercurous chloride.

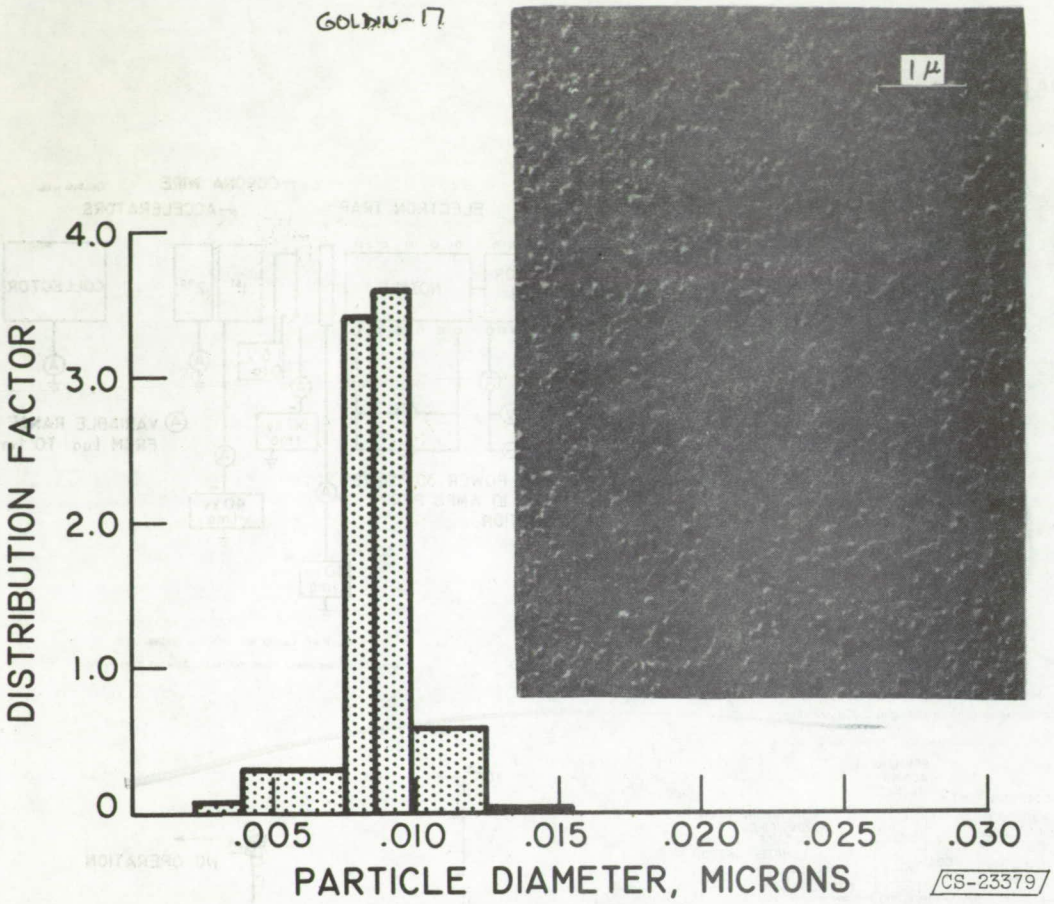

Figure 10. - Micrograph and particle distribution of mercurous chloride.

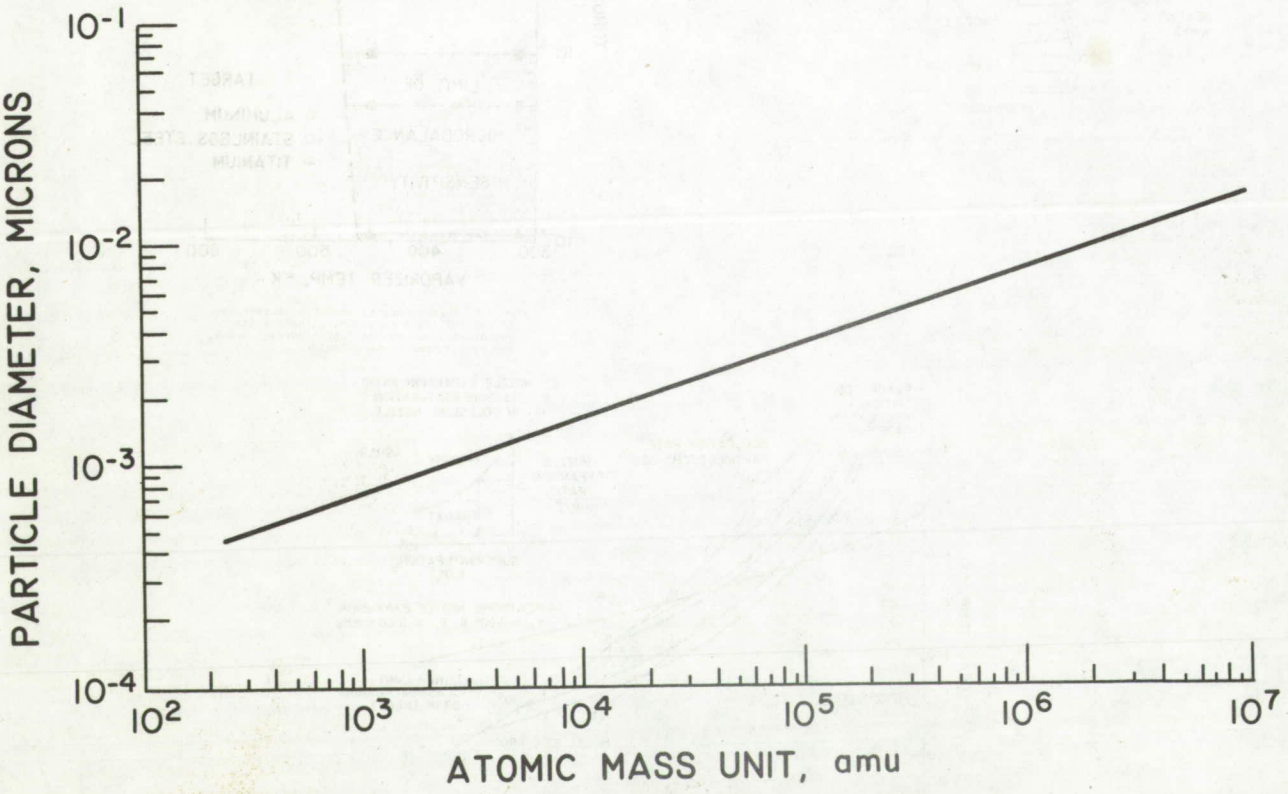

Figure 11. - Conversion of particle diameter to atomic mass units. Propellant, mercurous chloride.